

Impact of the Subsurface Structures on the Groundwater Occurrence in the Southeastern Part of Wadi El-Farigh, West Nile Delta, Egypt.

Ahmed M.A.H. Youssef
Desert Research Center, EL-Matareya, Cairo, Egypt.

The study area is bounded by the latitude of Khasm El-Kalb from the east and to the west of SUMID LINE from the west and extends between km 56 and km 67 along Cairo-Alex. Desert Highway. The structural setting prevailing the concerned area plays an important role in the levels of the basaltic sheet, which consequently has a direct effect on the groundwater occurrence. This basaltic sheet is overlain by the unconfined Lower Miocene aquifer (Moghra Formation) and is underlain by the confined Oligocene aquifer.

The present study deals with the subsurface geological structures and their direct effect on the vertical and horizontal distribution of the water bearing formations. To achieve the aim of this study, a geoelectrical study was carried out through the conducting of 36 Vertical Electrical Soundings (VES) with a maximum current electrode separation of 4000m of Schlumberger configuration. Also, the available data of 22 drilled wells was used in this study.

This study reveals the presence of 4 main geoelectrical layers. These layers, from top downward are: dry layer "A", an upper waterbearing layer "B" which is represented by Moghra formation, Oligocene basaltic sheet "C" and the lower water bearing layer "D" of Oligocene sediments.

The area is affected by a number of NE-SW and NW-SE faults which are detected through the correlation of the basaltic sheet levels. These faults have a great effect on the groundwater occurrence, as well as, on the connection and disconnection of Moghra and Oligocene aquifers in the investigated area.

Keywords: Groundwater – structures – Aquifer – Miocene – Oligocene – Vertical Electrical Soundings (EVS) – Geomorphology – Geology – Faults – Graben – horst

The significant increase in population has increased the necessity for further land reclamation which increases the demand for groundwater. The West Nile Delta including the study area has received the attention of both governmental as well as private sector for new land

reclamation activities, where groundwater and suitable soil are available besides its vicinity to Cairo.

Some problems were faced the investments at some farms, *e.g.* the farms of El-Berr Company closed to Khasm El-Kalb at the northeastern periphery of wadi El-Farigh and Green October Company at the southwestern periphery of wadi El-Farigh. These problems are the presence of the basaltic sheet at shallow depths below the water levels by few meters, the overlying thickness of the Moghra waterbearing formation is not suitable for exploitation, the presence of clay bed on the top and bottom boundary of the basaltic sheet and the necessary penetration of the basaltic sheet for exploitation of the underlying highly saline Oligocene aquifer. Consequently, the subsurface structures that affected on the subsurface distribution of the Moghra waterbearing formation (Miocene aquifer) which overlying the basaltic sheet had to be determined to find out the largest thickness for drilling water wells.

The study area (Fig. 1) lies between longitudes $30^{\circ} 37.5' E$ and $30^{\circ} 52.5' E$ and latitudes $30^{\circ} 08' N$ and $30^{\circ} 17.5' N$ covering an area of about 375 km^2 . It bounded by the latitude of Khasm El-Kalb from the east and to the west of SUMID LINE from the west and extends between km 56 and km 67 along Cairo-Alex. Desert Highway.

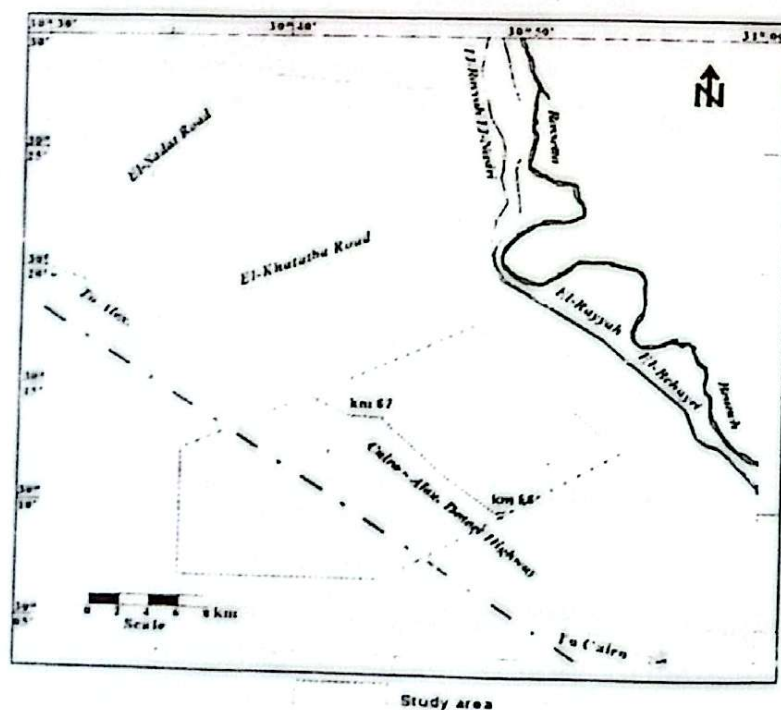


Fig. 1. Location map of the study area.

Geomorphological Features

The West Nile Delta area, including the investigated area lies within the arid province of Egypt. Its climate is characterized by long hot summer and short mild rainy winter. The southern part of the West Nile Delta area is characterized by a slightly undulated land surface that generally slopes towards the Northwest. A number of alternating ridges and depressions can also be recognized. These ridges are: Garet El-Haddadien plateau (+233m) and Gebel Hamza (+110m), while the depressions are represented by Wadi El-Farigh (-4m) and Wadi El Natrun (-23m). Generally, the southern part of the West Nile Delta area is covered by aeolian sand and gravels with occasional clay interbeds of Holocene and Pleistocene deposits (Said, 1962 and Abdel Baki, 1983).

Geological and Hydrogeological Setting

According to different authors such as: Said (1962), Shata *et al.* (1962), Shata and El Fayoumy (1967) and El Shazly *et al.* (1975), the West Nile Delta area is covered by sedimentary succession ranging in age from Late Cretaceous to Quaternary. Quaternary deposits are composed of sand, gravel and clay, followed by Miocene deposits of Moghra formation which is composed of coarse sand, clay and sandstone interbeds with vertebrate remains, silicified woods and gravels at base. The Miocene is underlain by Oligocene deposits of sand, sandy clay, clayey sand, clay, ferruginous sandstone, and sandy gravels. The Oligocene basaltic sheet is detected at some parts at depths ranging between 77m and 228m having maximum thickness of 30m. The basaltic sheet used as a marker bed in detecting the subsurface structures.

Based on the study carried out by many authors as Shata (1953), Said (1962), El-Shazly *et al.* (1975), El-Fayoumy (1964), Omara and Sanad (1975), El-Ghazawi and Atwa (1994) and Abd El-Rahman (1996), the area was affected by folds and normal faults.

Fold systems: The area is affected by two main fold systems of Syrian arc system (NE-SW) as Abu Roash anticline and the Clysmic system (NW-SE) which is represented by Wadi El-Farigh and Wadi El-Natrun anticlines.

Fault systems: The faults are mainly distributed parallel to the folds belonging to two fault systems. The first is the NE-SW (Aqaba system) as those faults which bounded Wadi El-Farigh from the north and the south, Gebel Hamza fault and Ras El-Hodhod – Gebel El-Mansouria fault. The other fault system belongs to the NW-SE (Clysmic system) and is represented by Garet El-Nagar and Khasm El-Kalb faults. These faults have a direct effect on lateral and vertical changes of the thickness of the Miocene aquifer.

Hydrogeologically, in the investigated area, the groundwater occurs through an upper unconfined aquifer of Moghra Formation (Miocene aquifer) and a lower one of confining nature (Oligocene aquifer). These aquifers are separated by the basaltic sheet

Abd El-Rahman (1996) carried out geophysical studies to the east of Cairo-Alex. Desert Highway between Abu Roash and El-Khatatba road. His study revealed the presence of 17 normal faults dissected the area in NE-SW and NW-SE trends. On the other hand, the present study is carried out to complete the picture of these structures on the western side of Cairo-Alex. Desert Highway along Wadi El-Farigh and at the same time using the available data of the new drilled wells to put the general structural forms along the southeastern part of Wadi El-Farigh on the eastern and western sides of Cairo-Alex. Desert Highway.

Geoelectrical Studies

Field work:

A total of 36 Vertical Electrical Soundings (V.E.S.) were carried out in the investigated area (Fig.2), where some of these soundings were conducted beside drilled wells to make an accurate interpretation. The Schlumberger configuration was applied with a distance between the two current electrodes starts from 2 meters and reaching 4000 meters. The Terrameter SAS 300 resistivity meter was used for measuring the resistance "R". Also, the available data of 22 wells were used in this study.

Topographic land survey has been carried out to find the accurate location and altitude of the sounding stations and the well sites.

Interpretation of the field data:

The quantitative interpretation of the measured field curves was carried out using a computer program "Resist" written by Vander

Velpen (1988) for non-automatic iteration method in which the field data are compared with data calculated from an assumed layer model. In the construction of such model, the bore hole data in the form of electrical and lithological logs and the available information about the regional and local geologic setting of the area were taken into consideration. An advantage of applying initial model derived from well data is to minimize the effect of the principle of equivalence and suppression. To confirm the results of Vander Velpen program (1988), another advanced computer program "RESIXP - Plus", v. 2.39 (1996), was used. This program is an interactive, graphically oriented, forward and inverse modeling program for interpreting resistivity sounding data in terms of a layered model.

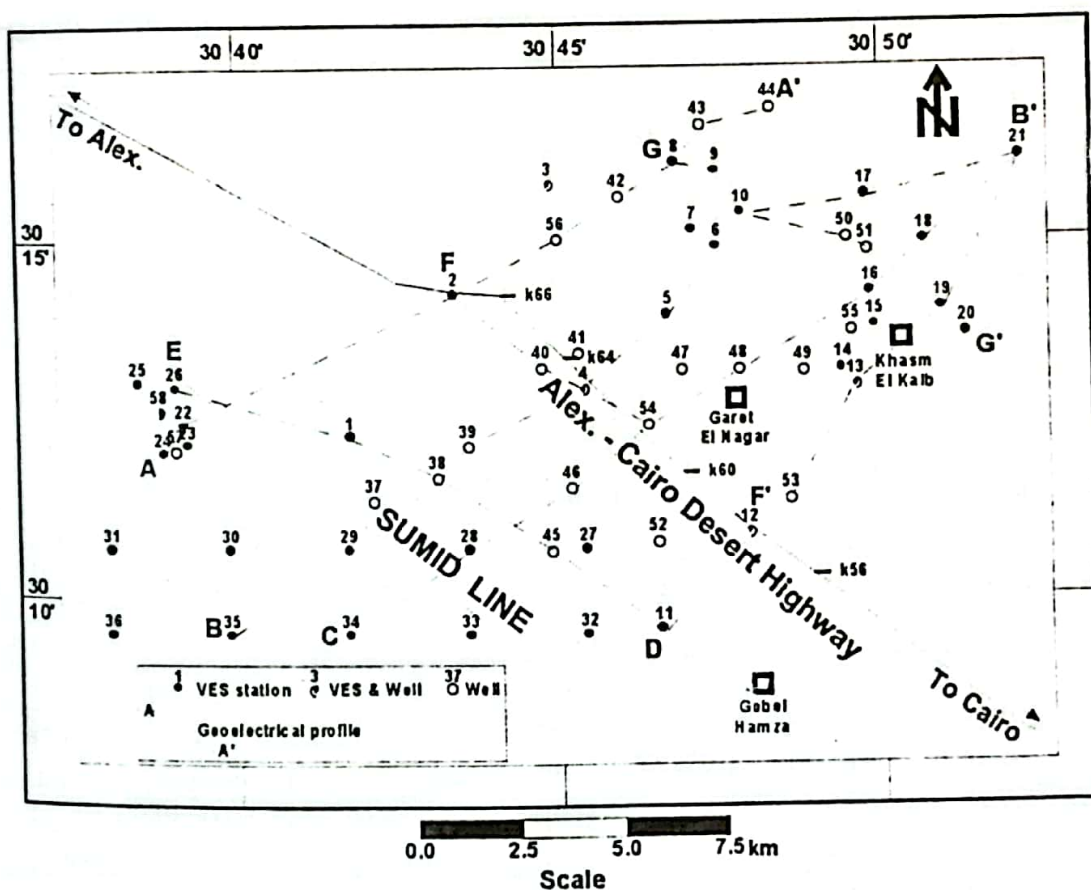


Fig. 2. Location map of the Vertical Electrical Sounding stations (VES), wells and geoelectrical profiles.

Discussion of the Geoelectrical Results

A- Geoelectrical succession:

The results of the quantitative interpretations are in the form of the resistivity and the corresponding thickness for each layer, which revealed the presence of 4 main geoelectrical layers. These layers from top downwards are: "A", "B", "C" and "D". Table (1), shows a description for each of these layers.

TABLE 1. Ranges of resistivities and thicknesses of the geoelectrical layers.

Geoelectrical layer	Resistivity	Thickness
"A"	22 Ohm-m @ VES No.8 – 5441 Ohm-m @ VES No.18	39.2 m @ VES No.35 – 103.61m @ VES No.25
"B"	9.7 Ohm-m @ VES No.17 – 105.5 Ohm-m @ VES No.15	14 m @ VES No.15 – 167 m @ Well No.41
"C"	250 Ohm-m @ VES No.6 – 984 Ohm-m @ VES No.14	22 – 30 m
"D"	1 Ohm-m @ VES No.26 – 43.7 Ohm-m @ VES No.14	----- --

1. *The first layer "A"*, is a summation of a number of sublayers forming the unsaturated zone along the investigated area. Lithologically, it consists of dry gravel and sand with occasional clay intercalations. It exhibits a great range of resistivity values (Table 1), ranging between 22 Ohm-m at VES No.8 and 5441 Ohm-m at VES No.18. These resistivities reflect the nature of this layer, where the presence of the clay intercalations decrease the resistivity. The thickness of this layer (Table 1), which represents the depth to water along the investigated area, ranges between 39.2m at VES No.35 to 103.61m at VES No.25.

2. *The second geoelectrical layer "B"*, represents the upper waterbearing layer consisting of Moghra Formation (Miocene aquifer). It consists of coarse sand, clay and sandstone interbeds with vertebrate remains, silicified woods and gravels at base. The resistivity of this layer (Table 1), ranges between 9.7 Ohm.m at VES No.17 and 105.5 Ohm.m at VES No.15. The decrease in the resistivity values reflect the increase of the clay content in the waterbearing formation. The thickness of this geoelectrical layer (Table 1) ranges between 14m at VES.No.15 and 167m at Well No.41. The base of this layer directly above the basaltic sheet consists of clay or sandy clay.
3. *The third geoelectrical layer "C"*, is represented by basaltic sheet of Oligocene age. This layer is not encountered in the whole investigated area. Its resistivity (Table 1) ranges between 250 Ohm.m at VES No. 6 to 984 Ohm.m at VES No.14. These resistivities reflect to a great extent the nature of the basaltic sheet, where the low resistivity is attributed to the presence of weathered and fractured basalt partially saturated with groundwater, whereas the high resistivity is related to the massive basaltic sheet. The thickness of this basaltic sheet is nearly uniform ranging between 22m and 30m (Table 1). This layer separates the overlying unconfined Miocene aquifer and the underlying confined Oligocene aquifer.
4. *The fourth and the last geoelectrical layer "D"*, was not detected at the whole investigated area, but only at some parts. It represents the second waterbearing formation (Oligocene aquifer). It consists of sand, sandy clay, clayey sand, clay, ferruginous sandstone and sandy gravels. The resistivity of this layer (Table 1) ranges between 1 Ohm.m at VES No.26 to 43.7 Ohm.m at VES No.12. Comparing the resistivity values of this layer by that of layer "B" (9.7-105.5 Ohm.m), it is noticed that the low resistivity values of layer "D" (Oligocene aquifer) is attributed to an increase of clay content as well as an increase of water salinity, which is confirmed by the well logging data at a drilled well between VES Nos.23 and 24 (Fig. 3). The top of this layer, which directly below the basaltic sheet, consists of clay or sandy clay.

B- Geoelectrical cross sections:

The areal distribution of the geoelectrical layers and the subsurface structures can be clearly identified through the constructions of 7 geoelectrical cross sections. Four of them (AA', BB', CB' and DB'), were constructed in SW-NE direction (Figs. 4-7), and the others (ED, FF', and GG) taking NW-SE directions (Figs.8-10). This will help in detection of any faults taking the prevailing fault systems; with its NE-SW direction and NW-SE trend.

To avoid unnecessary repetitions, the main observations and conclusions from these sections can be summarized as follows:

1. The geoelectrical layers "A" and "B" are represented along the investigated area, while the other two layers "C" and "D" are encountered only at some parts in the investigated area, because they were neither reached by the soundings nor by the drilling due to their presence at deep depths.
2. The geoelectrical cross sections (Figs. 4-10) show that Wadi El-Farigh and its vicinities are affected by 8 normal faults with NW-SE trend and 5 normal faults having NE-SW trend.
3. These faults with each others make alternative high structures (horst) and low structures (graben).
4. The dissecting of the basaltic sheet along the different geoelectrical cross sections by numerous faults has brought the faulted basalt blocks at different levels which resulted in a direct hydraulic connection between the Lower Miocene aquifer, that overlying the basaltic sheet and the Oligocene aquifer, that underlying the basaltic sheet.

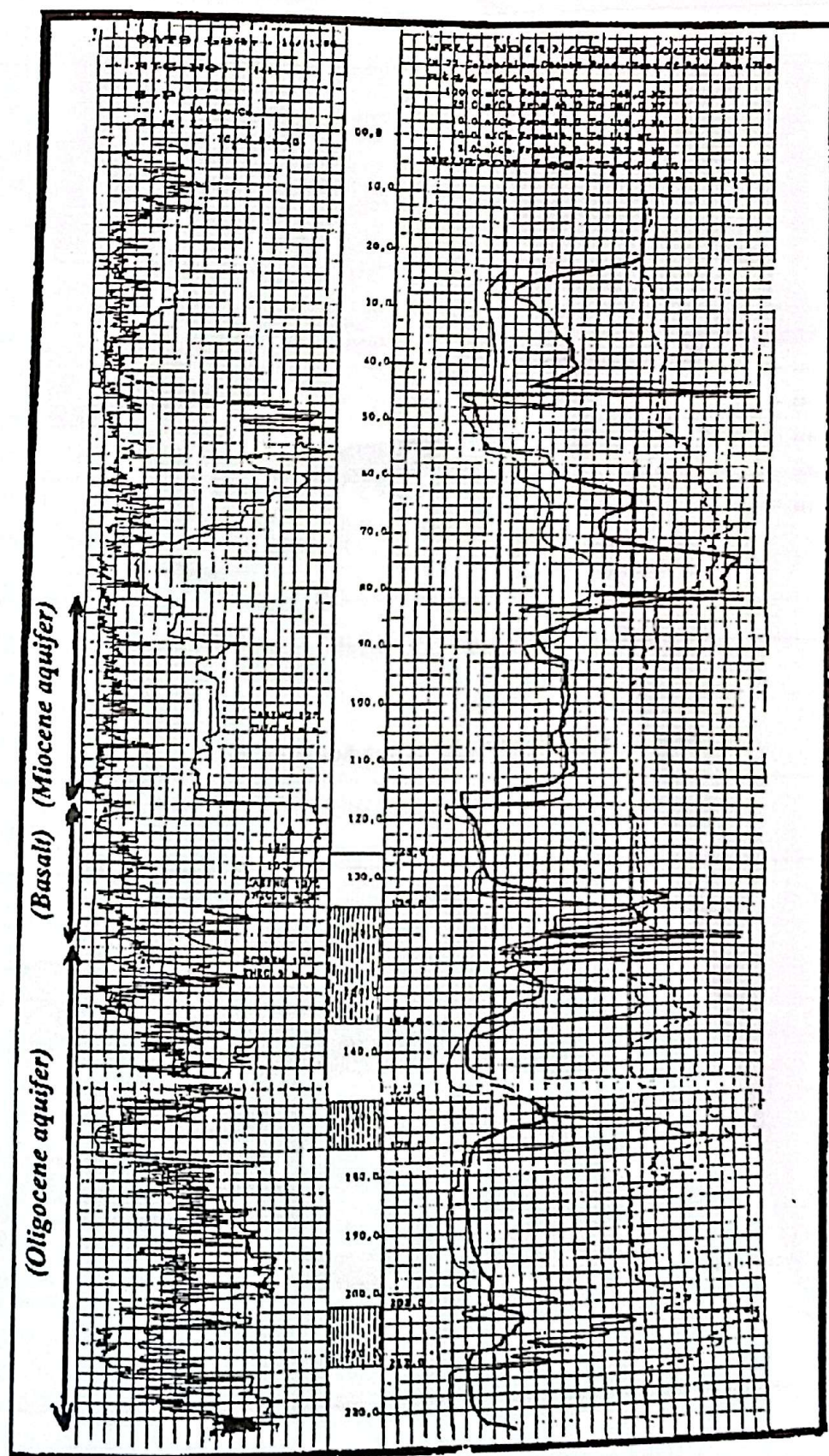


Fig. 3. Electrical well logging of well No. 58.

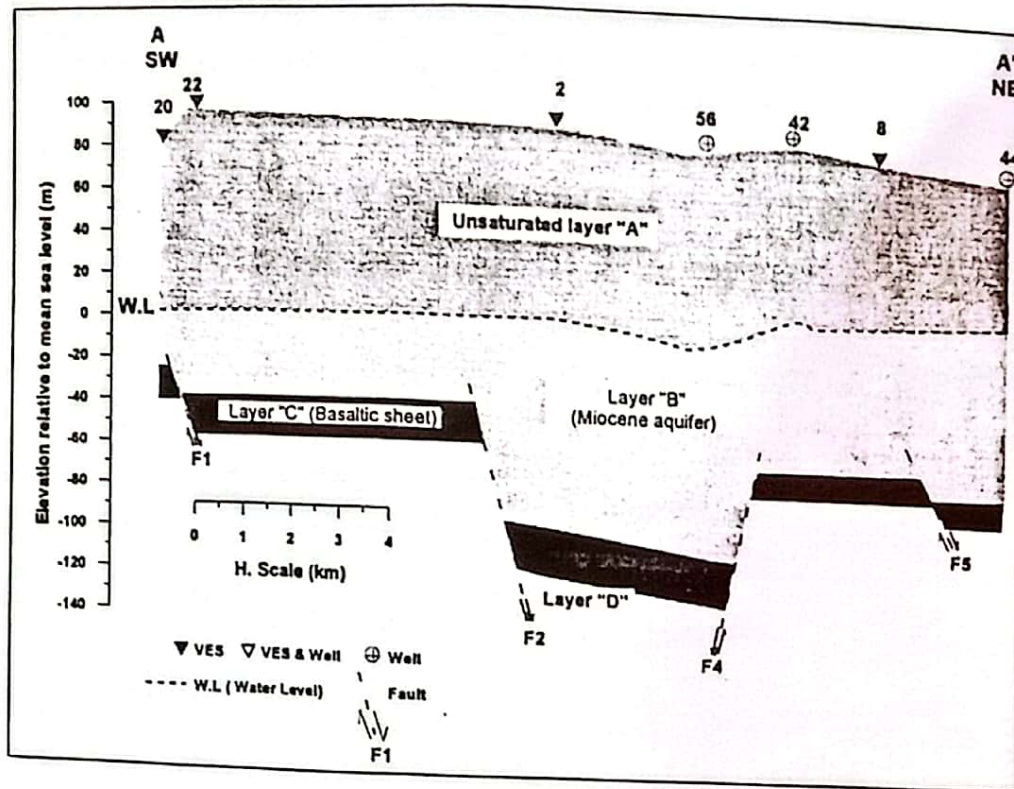


Fig. 4. Geoelectrical cross section A-A'.

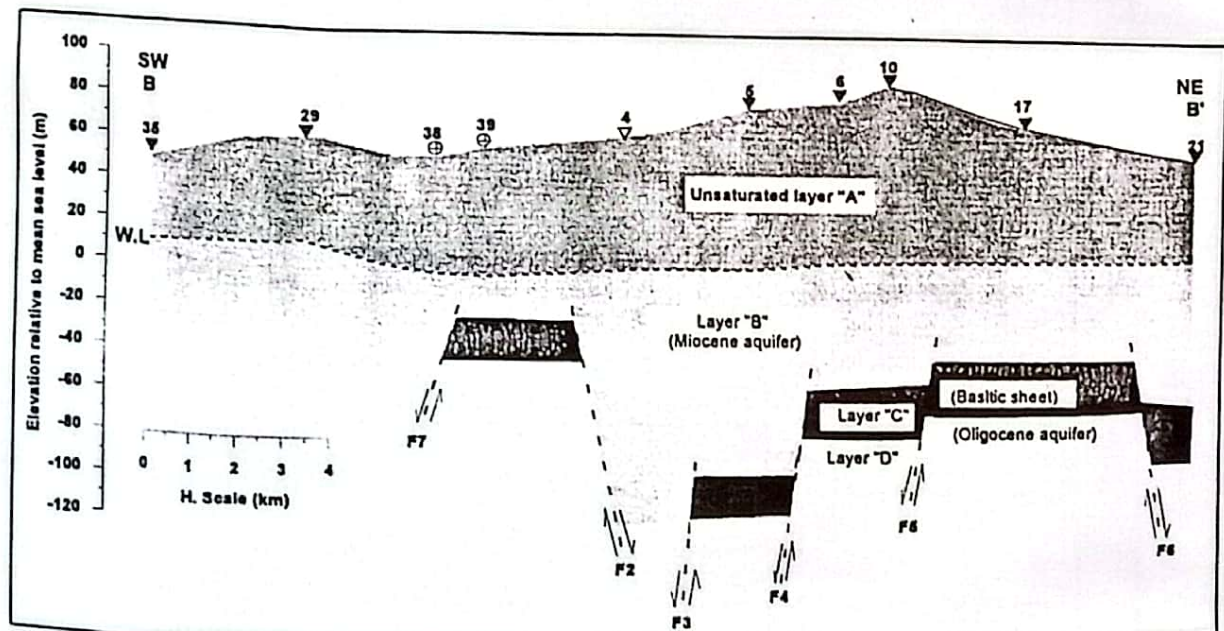


Fig. 5. Geoelectrical cross section B-B'.

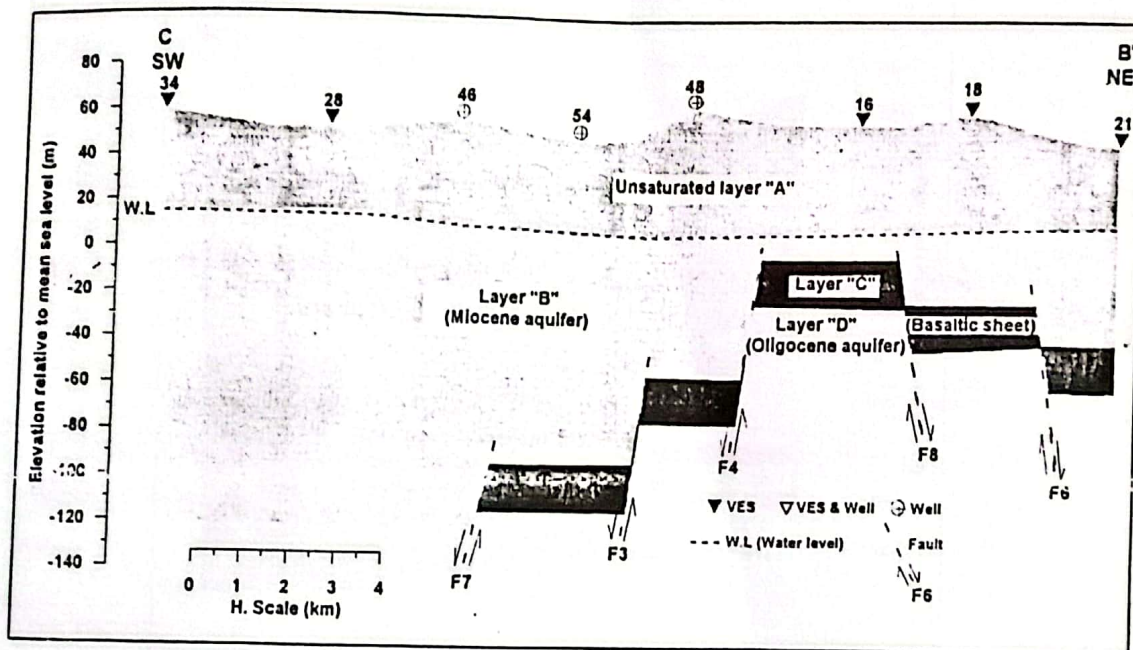


Fig. 6. Goelectrical cross section C-B'.

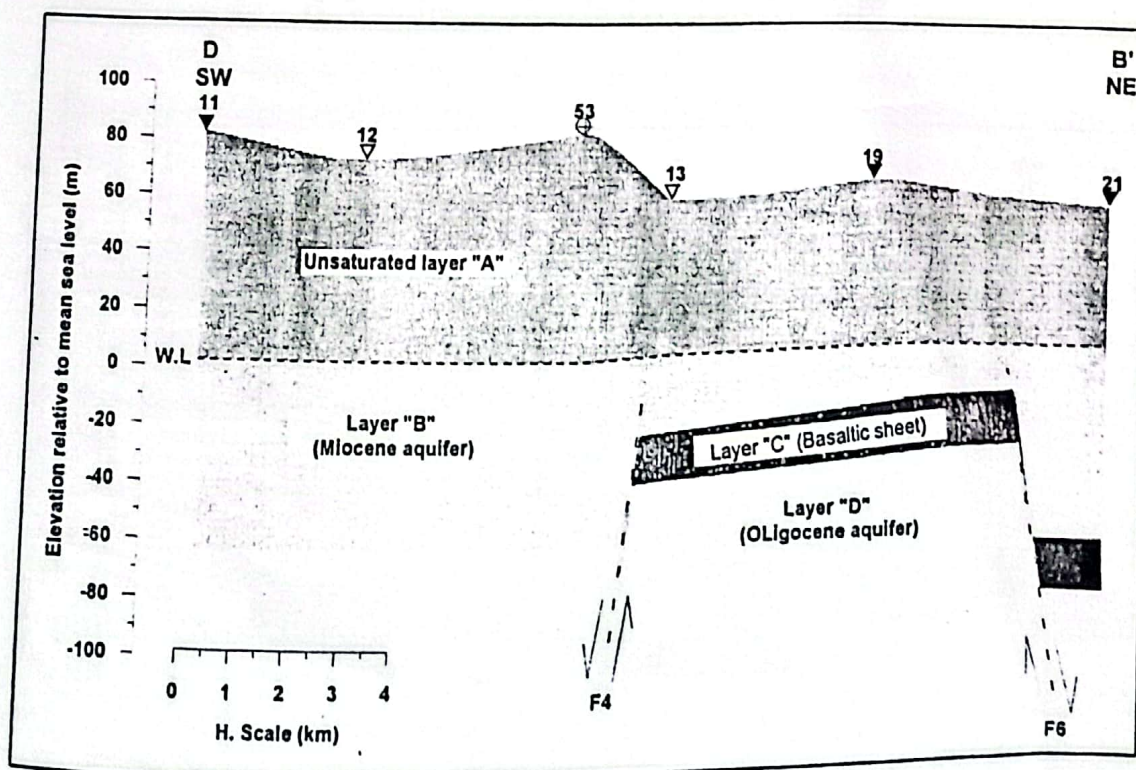


Fig. 7. Goelectrical cross section D-B'.

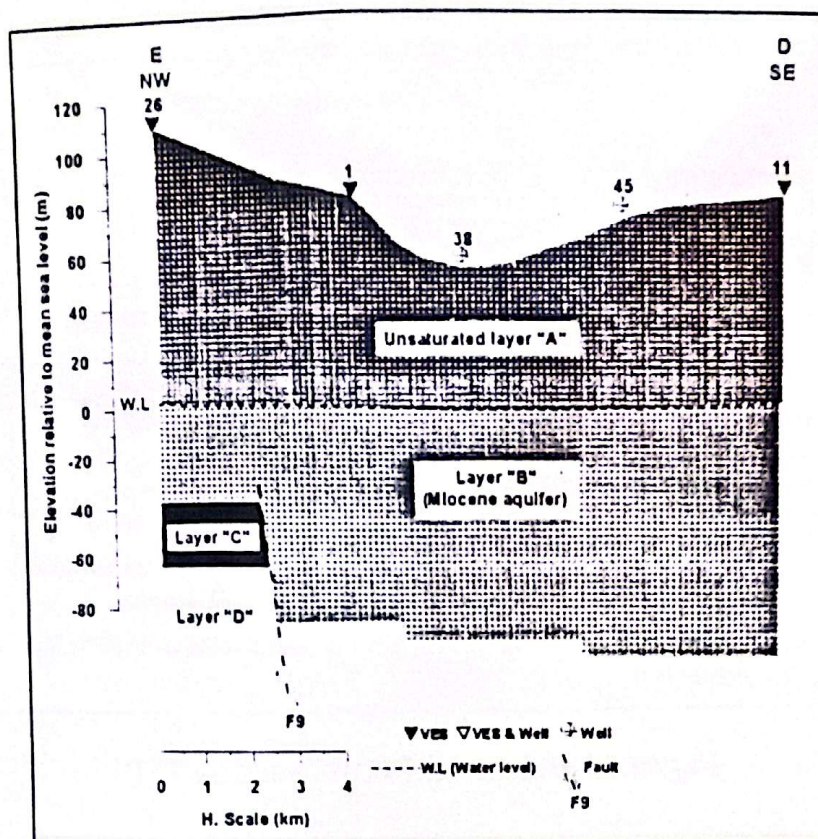


Fig. 8. Geoelectrical cross section E-D.

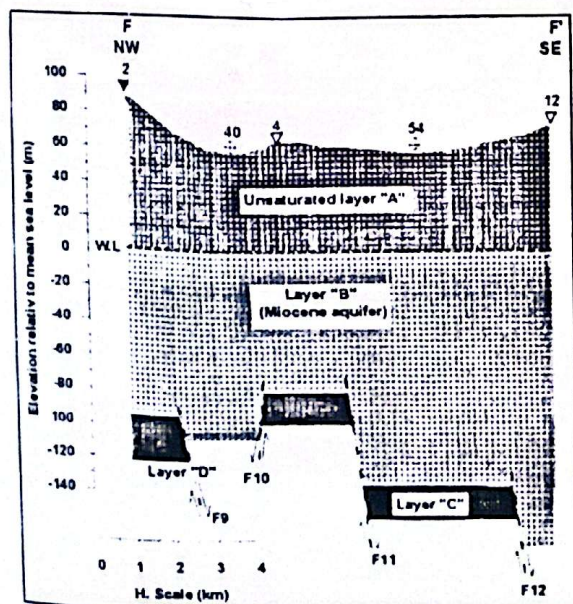


Fig. 9. Geoelectrical cross section F-F'.

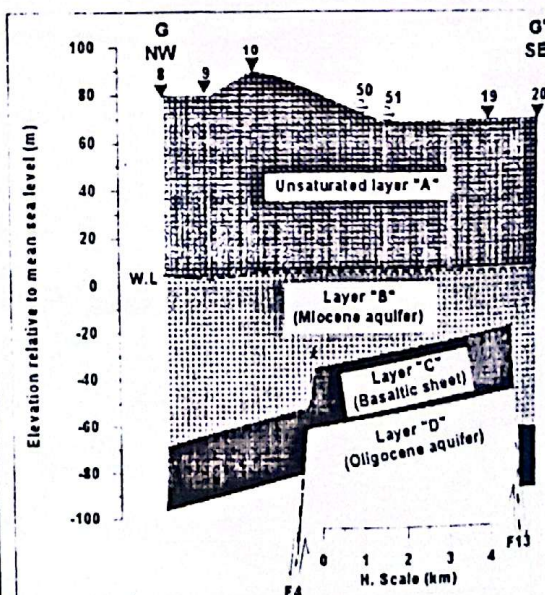


Fig. 10. Geoelectrical cross section G-G'.

Groundwater Occurrence

The Miocene and Oligocene sediments are representing the main waterbearing formations in the investigated area, which are previously referred as the geoelectrical layers "B", and "D", separated by the Oligocene basaltic sheet (Layer "C"). The average water salinity of the Miocene aquifer ranges between 281.6 mg/l near the Rosetta Branch and 823 mg/l at the western portion of the study area, while, that of the Oligocene aquifer is 2566 mg/l (El Ghazawi and Atwa, 1994).

The investigated area as a part of the West Nile Delta has been suffered from intensive fault systems, accordingly these faults have its direct contribution on the groundwater occurrence.

Through this part, the factors that controlled the groundwater occurrence will be discussed. These factors include; thickness of the waterbearing formation, depth to water, groundwater flow, distribution of the basaltic sheet and the impact of the detected faults on the groundwater occurrence.

Thickness of waterbearing formation (Layer "B"):

The distribution of the thickness of the upper waterbearing formation (Moghra Formation), that is represented by the geoelectrical layer "B" (Miocene aquifer) can be illustrated through the isopach contour map (Fig.11). This map shows that, its thickness ranges between 14m at VES 15 and 167m at Well No.41. The lower boundary of the Miocene aquifer is defined by the underlying basaltic sheet. The faults are the main factors controlled the thickness of the Miocene aquifer. As shown in Figure (12) and the geoelectrical cross sections (Figs. 4-10), it is clear that the aquifer has its maximum thickness in the downthrown side of the step faults as well as in the graben-like which is clear in the center of the map around Cairo-Alex. Desert Highway. On the other hand, the minimum thickness presents at the uplifted areas (horsts) as clear in the northeastern portion at Khasm El Kalb.

Depth to water and groundwater flow:

The depth to water is mainly related to topography, where the shallowest depth to water is recorded at the lowest elevated land. However, it ranges between 39.2m at VES No.35 and 108.04m at

VES No.26 with general increase towards the northwest and southeast.

The groundwater flow of the Miocene aquifer can be illustrated through the construction of the water level contour map with respect to the mean sea level (Fig. 12). The water level ranges between -6.88m at well No.56 and 6.51m at VES No.21. The water flow takes the general flow of the West Nile Delta area from the east and northeast towards the west and southwest. The water level reaches -6.88m making a cone of depression near Cairo-Alex. Desert Highway at km 66, which is a serious result of the high rate of water extraction in that area and consequently will cause water depletion of the aquifer.

Basaltic sheet:

As mentioned before, the basaltic sheet is affected by the normal faults in the investigated area and consequently has a direct controlling on the thickness of the Miocene aquifer.

Figure (13) illustrates a contour map of the depth to basalt. This depth ranges between 80.75m at VES No.16 and 228m at Well No.41.

The depth to the basalt has its maximum values on the graben-like, whereas the minimum depth is recorded at the uplifted parts at Khash El Kalb.

The abrupt variation in the depth to basalt is due, mainly, to the different faults that had affected the basaltic sheet. This can be further clarified through the construction of a structure contour map for the upper surface of the basaltic sheet (Fig. 14). This map shows that, the level of the basaltic sheet ranges between -12.69m at VES No 16 and -159.64m at VES No.41

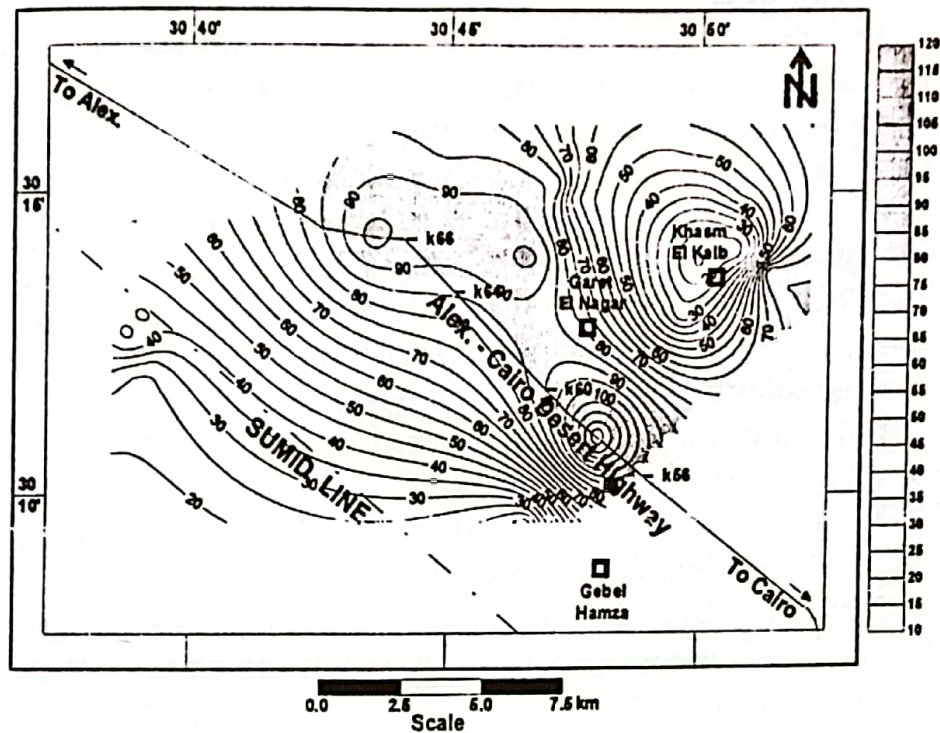


Fig. 11. Isopach map of the waterbearing Moghra Formation (Miocene aquifer).

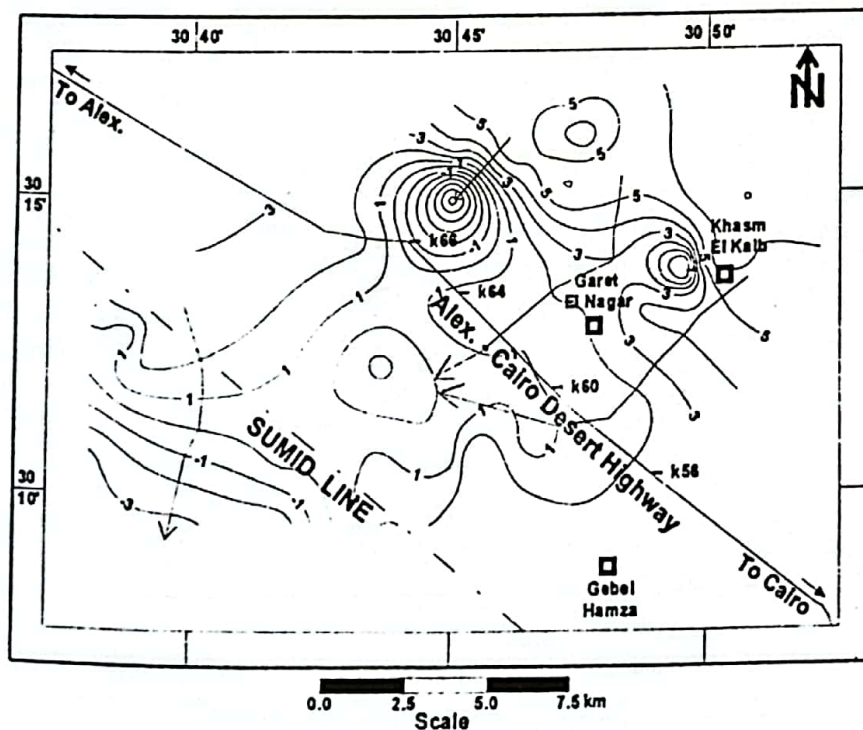


Fig. 12. Water level contour map.

Inferred structures:

The basalt level contour map (Fig.14) and the constructed geoelectrical cross sections (Figs.4-10) revealed that the investigated area had been subjected to intensive movements that resulted in dissecting the area with 13 normal faults having NE-SW and NW-SE trends (Fig. 15). Some of these faults are confirmed by that detected by Abd El Rahman (1996) and the others are newly detected including, F1, F7, F9, F10, F11 and F12, which complete the general structural pattern along the southeastern part of Wadi El Farigh on the east and west sides of Cairo-Alex. Desert Highway.

From the map of the inferred faults (Fig.15) and the constructed geoelectrical cross sections (Figs.4-10), it is clear that the NW-SE fault system dissected Wadi El Farigh from the southwest to the northeast making low structures (grabens) between F1&F7, F2&F4 and alternative high structures (horsts) between F7&F2 and F4&F6. Also, the highest uplifting (horst) takes place at Khash El Kalb, which indicated by the high level of the basaltic sheet, then through the step faults with their downthrown sides towards the northeast and southwest, the basaltic sheet goes deep.

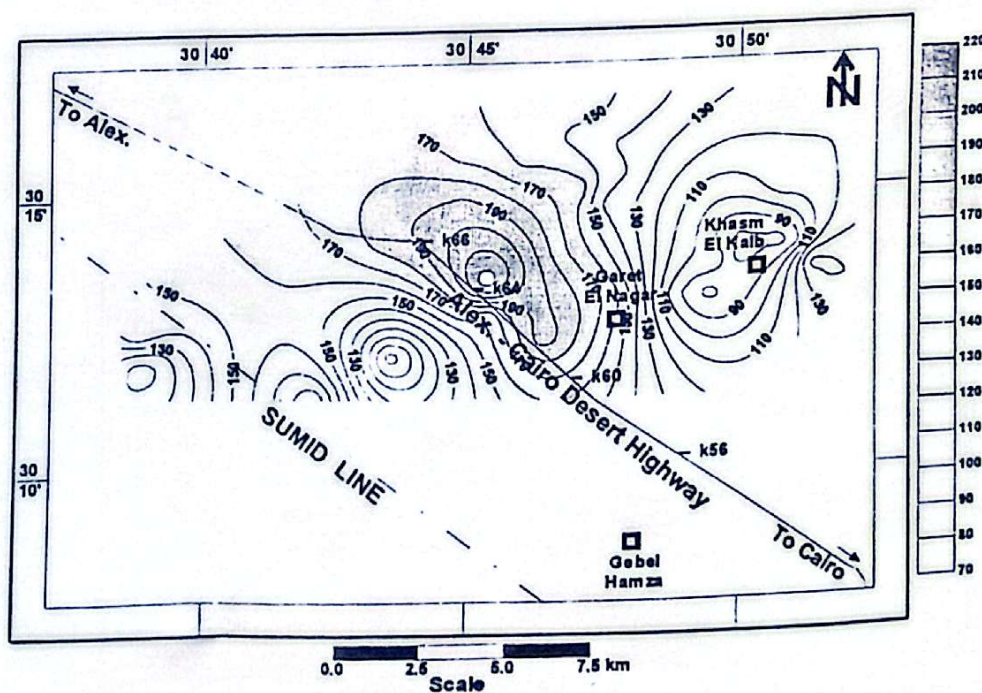


Fig. 13. Depth to basalt contour map.

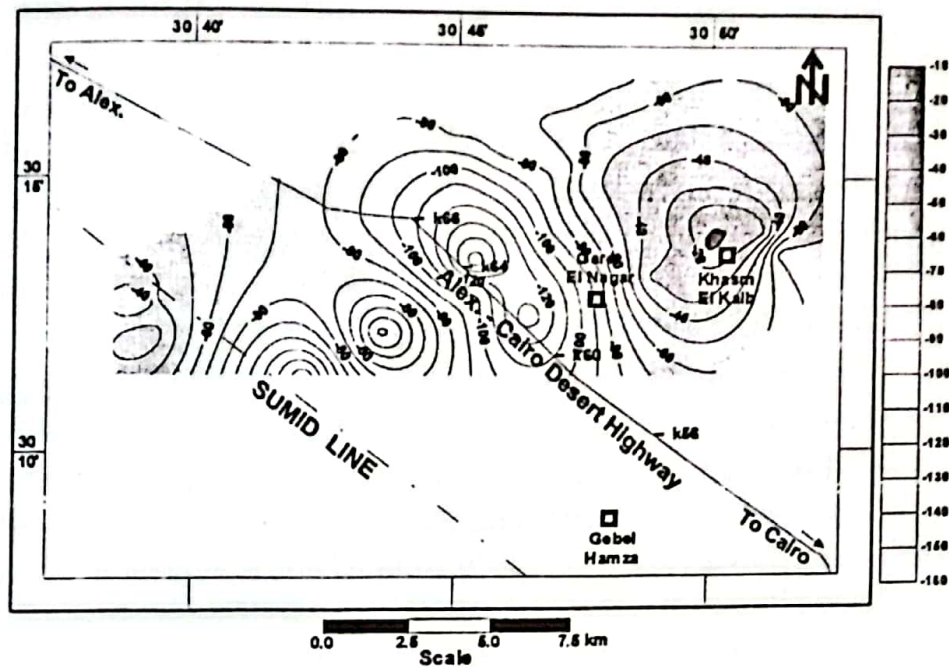


Fig. 14. Structure contour map for the upper surface of the basaltic sheet.

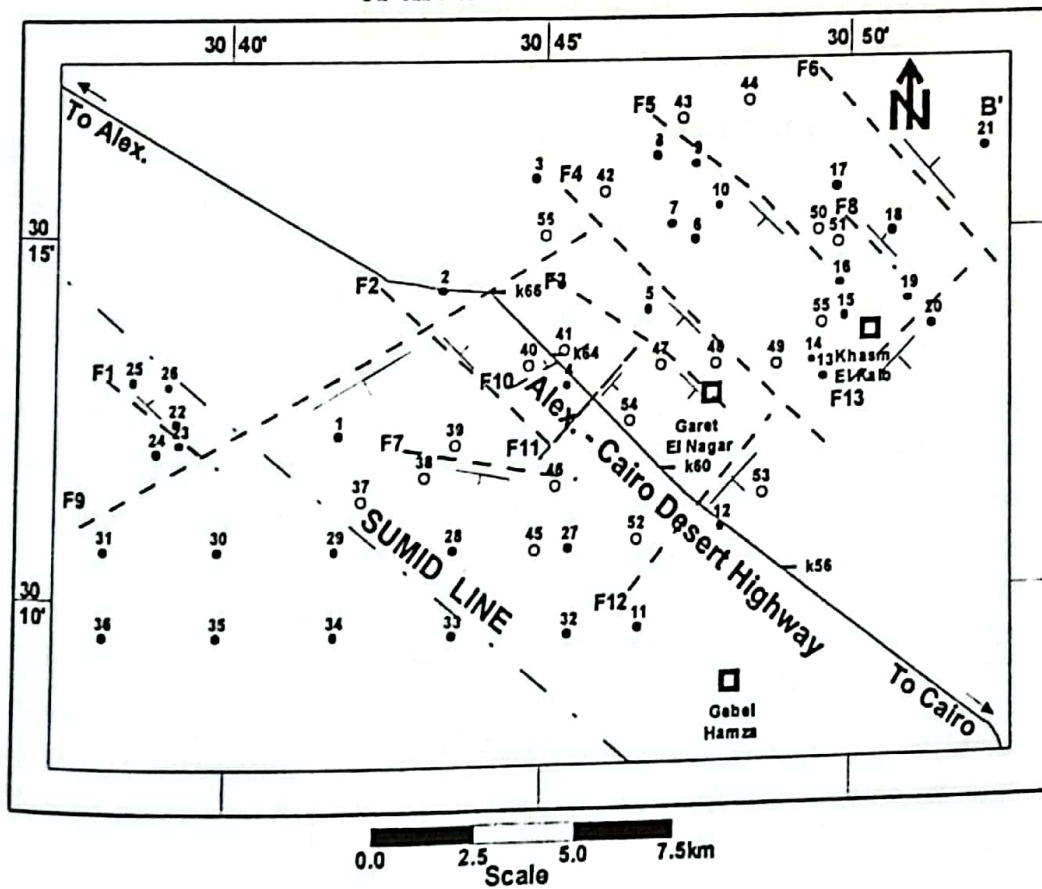


Fig. 15. Inferred fault map.

From the map of the inferred faults (Fig.15) and the constructed geoelectrical cross sections (Figs.4-10), it is clear that the NW-SE fault system dissected Wadi El-Farigh from the southwest to the northeast making low structures (grabens) between F1&F7, F2&F4 and alternative high structures (horsts) between F7&F2 and F4&F6. Also, the highest uplifting (horst) takes place at Khash El-Kalb, which indicated by the high level of the basaltic sheet, then through the step faults with their downthrown sides towards the northeast and southwest, the basaltic sheet goes deep.

The impact of these faults on the groundwater occurrence in the investigated area can be clarified as follows:

- The high structures (horsts), resulted in uplifting the basaltic sheet, which consequently decreases the thickness of the overlying Lower Miocene aquifer, this is evident by the smallest thickness of the Miocene aquifer at Khash El-Kalb (14m at VES 15). On the other hand, the low structures (graben), resulted in brought the basaltic sheet at great depth, which consequently increases the thickness of the overlying Lower Miocene aquifer (167m at Well No.41).
- On the high structures (horsts), the small thickness of the Lower Miocene aquifer is not enough for exploitation, so the basaltic sheet should be penetrate to reach the Oligocene aquifer which has high water salinity. On the low structures (graben), a sufficient thickness of the Lower Miocene aquifer presence overlying the basaltic sheet, and consequently, the drilling will be stop on the upper surface of the basaltic sheet.
- The NE-SW fault system which striking parallel to the groundwater flow, accelerate the water movement and act as conduits, and also, it affects the hydraulic gradient.
- The dissecting of the basaltic sheet by these faults, has brought the faulted basalt blocks at different levels, which resulted in a direct hydraulic connection between the Lower Miocene aquifer (overlying basaltic sheet) which has low salinity and the Oligocene aquifer (underlying the basaltic sheet).

Conclusion

The application of the electrical resistivity sounding method in a part of Wadi El-Farigh with the purpose of delineating the geologic structures and its impact on the groundwater occurrence has revealed the following:

1. The geoelectrical succession down to a depth of about 250m consists of 4 geoelectrical layers:

The first geoelectrical layer "A", forms the unsaturated zone consisting of gravel, sand with occasional clay intercalations. It exhibits a great range of resistivity values (22-5441 Ohm-m) and its thickness is 39.2-103.61m, which represents the depth to water along the investigated area.

The second geoelectrical layer "B", represents the upper waterbearing formation (Miocene aquifer). It consists of coarse sand, clay and sandstone interbeds with vertebrate remains, silicified woods and gravels at base. Its resistivity is 9.7-105.5 Ohm.m. and has thickness between 14 m 167m.

The third geoelectrical layer "C", is represented by basaltic sheet of Oligocene age. It has resistivity 250-984 Ohm.m and has a uniform thickness between 27m and 30m.

The fourth and the last geoelectrical layer "D", was not detected at the whole investigated area, but only at some parts. It represents the second waterbearing formation (Oligocene aquifer). It consists of sand, sandy clay, clayey sand, clay, ferruginous sandstone and sandy gravels. Its resistivity varies from 1 to 38 Ohm.m.

2. The geoelectrical cross sections (Figs. 6-12) show that Wadi El-Farigh and its vicinities are affected by 8 normal faults with NE-SW trend and 5 normal faults having NW-SE trend. These faults with each other making alternating high structures (horst) with small thickness of the Lower Miocene aquifer and low structures (graben) with great thickness of the Lower Miocene aquifer.
3. The dissecting of the basaltic sheet along the different geoelectrical cross sections by numerous faults has brought the faulted basalt blocks at different levels which resulted in a direct hydraulic connection between the Lower Miocene aquifer, that

overlying the basaltic sheet and the Oligocene aquifer, that underlying the basaltic sheet.

Recommendations

1. The hydraulic connection between the Lower Miocene aquifer and the Oligocene aquifer, by continuous pumping, the Miocene water will be affected by the more saline water of the Oligocene aquifer.
2. The haphazard drilling in the investigated area will affect on the quantity and quality of the groundwater in the future.
3. The great numbers of drilled wells nowadays will extract more water, which consequently, result in make depletion to the groundwater level and increase the water salinity.
4. Accordingly, the drilling process should be under the control of the government.

Acknowledgement

The author is gratefully indebted to the head and the staff members of the Geophysical Exploration Department, Desert Research Center, for their agreement of using the field data.

References

- Abd El-Baki, A.A. (1983).** Hydrogeological and hydrogeochemical studies on the area west of Rosetta Branch and south of El-Nasr Canal.", *Ph.D Thesis*, Fac. Sci., Ain Shams Univ., Cairo, Egypt.
- Abd El-Rahman, A.A. (1996).** Geophysical study on the groundwater conditions in the area southwest of the Nile Delta between Abu Roash and El-Khatatba road., *M.Sc. Thesis*, Fac. Sci., Ain Shams Univ., Cairo, Egypt. 116p.
- El-Ghazawi, M.M. and Atwa, S.M. (1994).** Contribution of some structural elements to the groundwater condition in the southwestern portion of the Nile Delta. *Egypt. J. Geol.*, **38**(2), p 649-667.
- El-Fayoumy, I.F. (1964).** Geology of groundwater supplies in Wadi El Natrun area., *M.Sc. Thesis*, Fac. Sci., Cairo Univ., Cairo, Egypt.

- El-Shazly, E.M.; Abdel Hady, M.A.; El Ghawaby, M.A.; El Kassas, I.A.; Khawasik, S.M.; El Shazly, M.M. and Sanad, S. (1975). Geologic interpretation of landsat satellite images for West Nile Delta area, *Remote Sensing Center, Academy of Scientific Research and Technology, Cairo, Egypt*, 38.pp
- INTERPEX Limited (1996). "RESIXP - PLUS, Resistivity data interpretation software, v. 2.39", Golden, Colorado, U.S.A.
- Omara, S.M. and Sanad, S. (1975). Rock stratigraphy and structural features of the area between Wadi El-Natron and the Moghra depression, Western Desert, Egypt., *Geol. Jb, B1,6, Hanover.*, p 45-73.
- Said, R. (1962). "*The Geology of Egypt*", Elsevier Pub. Co., Amsterdam.
- Shata, A.A. (1953). New light on the structural developments of the Western Desert of Egypt, *Bull. Inst. Desert d'Egypt*, T.III, No.1, p 101-106.
- Shata, A.A. and El-Fayoumy, I.F. (1967). "Geomorphological and morphopedological aspects of the region west of the Nile Delta with special reference of Wadi El-Natron area", *Bull. Inst. Desert d' Egypt*, T. III, No.1, p 1-28
- Shata, A.A.; Pavlov, M. and Saad, K.F. (1962). Preliminary report on the geology, hydrogeology and groundwater hydrology of Wadi El-Natron and adjacent areas., *Internal Report, Desert Inst., Cairo, Egypt*.
- Vander Velpen, B.P.A. (1988). "RESIST", version 1.0, a package for the processing of the resistivity sounding data, M. Sc. Thesis Research Project, ITC, Delft, the Netherlands.

Received 21/6/2000

Accepted 1/8/2000

تأثير التراكيب التحت سطحية على تواجد المياه الجوفية في الجزء الجنوبي الشرقى من وادى الفارغ - غرب دلتا النيل - مصر .

أحمد محمد على يوسف

مركز بحوث الصحراء - المطرية - القاهرة - مصر

إن التراكيب الجيولوجية فى منطقة الدراسة لها دور هام فى ظروف تواجد المياه الجوفية . ومدى الاتصال الهيدروليكي بين خزان الميوسين السفلى الممثل برواسب المغرة والذي يعلو شرائح البازلت الموجودة بالمنطقة وخزان الألوجوسين الذى يوجد تحت البازلت .

تقع منطقة الدراسة بين خطى طول ١٧,٥ ٣٠ شرقاً و ٥٢,٥ ٣٠ شرقاً وخطى عرض ٨ ٣٠ شمالاً و ١٧,٥ ٣٠ شمالاً وتغطى مساحة حوالى ٣٧٥ كم^٢.

تهدف هذه الدراسة لتتبع مستوى شرائح البازلت وتحديد التراكيب المؤثرة عليها وتأثيرها على امتداد الخزانات الجوفية أفقياً ورأسياً . وللوصول الى هذا الهدف تم عمل عدد ٣٦ جسة كهربية رأسية وتم الاستعانة بمعلومات عدد ٢٢ بئر . ومن هذه الدراسة فإن التتابع الجيوكهربى يتكون من عدد ٤ طبقات جيوكهربية (أ ، ب ، ج ، د) .

الطبقة العليا " أ " تمثل الرواسب الجافة ، تحتها الطبقة " ب " وهى تمثل خزان الميوسين العلوى ، تحتها الطبقة " ج " ويمثلها البازلت والطبقة الأخيرة " ج " تمثل خزان الألوجوسين . ومن خلال عمل القطاعات الجيوكهربية وخريطة مستوى سطح البازلت

تم استنتاج أن المنطقة متأثرة بعدد من الفوالق فى إتجاه الشمال الشرقى - الجنوب الغربى والشمال الغربى - الجنوب الشرقى والتي أثرت على سمك خزان الميوسين مما أدى الى إمكانية استغلال هذا الخزان فى أماكن (السمك كبير) وعدم إمكانية إستغلاله فى أماكن أخرى (السمك ضئيل) ، وكذلك أدت هذه الفوالق الى الاتصال الهيدروليكي بين خزان الميوسين ذو الملوحة الأقل وخزان الألوجوسين المرتفع الملوحة .

وخلص البحث الى التوقف عن حفر الآبار العشوائى وأن يكون ذلك تحت سيطرة الجهات المعنية وأيضاً لابد أن تقنن معدلات كميات السحب الزائدة والتي تؤدى الى هبوط مستوى المياه وزيادة الملوحة .